Glasses with Medical Applications

María Vallet-Regí,*[a] C. Victoria Ragel,[a] and Antonio J. Salinas[a]

Keywords: Glasses / Materials science / Organic-inorganic hybrid composites / Metallic coatings / Textural properties

Bioactive glasses react chemically with the body fluids. The reaction product is an apatite, which, with the intervention of biological drivers, assists the generation of bone matrix and bone growth. The main application of these bioactive glasses in the clinical field is the filling of osseous cavities, manufacture of small parts for middle ear bone replacement and maxilofacial reconstruction and dental applications. Thanks to advances in related medical technologies, bioactive glasses are now undergoing a new stage of development, resulting in different mechanical properties, drug delivery capabilities, bioactive coating of metallic implants, protein and/or cell activation for tissue regeneration and tissue engineering, and are also finding use in biomimetics, nanotechnology, production of hybrid organic-inorganic materials and as bioactivity accelerators of mineral apatites or as bioactivity inductors of magnetic materials for hyperthermia treatment of osseous tumours.

1. Introduction

The discovery of the first *bioactive* ceramic took place 30 years ago, and since then has given rise to new strategies in the use of artificial materials in clinical bone repairs and replacement. The bioactive ceramics spontaneously bond to and integrate with living bone in the body without fibrous tissue forming around them. It was Hench et al.[1,2] who first introduced the idea of firmly bonding bone with synthetic materials through the chemical reactions that take place on a glass surface when it is implanted into a living body. Such an original line of thinking focussed attention on silica-based glasses, with the amorphous structure of silica glass, and on the chemical reactions that occurred on the surfaces of such materials. Bioglass® [1] and the subsequent family of bioactive glasses are now regarded, from the point of view of their application, as the earliest expression of all bioactive ceramics.

The characteristic amorphous quality of these glasses is generally a product of the structure of silicate glass, usually defined by [SiO_4] tetrahedra. These geometrical figures are linked together at all corners. While crystallised silica shows a uniform arrangement of these tetrahedra, as could be expected of any crystalline material (Figure 1, a), this is not

[a] Departamento de Química Inorgánica y Bioinorgánica, Facultad de Farmacia,
Universidad Complutense, 28040 Madrid, Spain
Fax: (internat.) + 34-91/394-1786
E-mail: vallet@farm.ucm.es

María Vallet-Regí (left, top) was born in Las Palmas, Spain, in 1946. She studied Chemistry at the Universidad Complutense de Madrid (UCM) and received her PhD at the same University in 1974. She is full professor of Inorganic Chemistry and Head of the Department of Inorganic Chemistry and Bioinorganic at the Faculty of Pharmacy (UCM). Her current research field is solid state chemistry, covering aspects of synthesis, characterisation and reactivity in oxides and bioceramics.

C. Victoria Ragel (right) was born in Madrid, Spain, in 1957. She studied Pharmacy at the Universidad Complutense de Madrid (UCM) and received her PhD at the same University in 1984. She was associate professor at the Department of Inorganic Chemistry and Bioinorganic at the Faculty of Pharmacy (UCM). In the last years, her research fields were the synthesis, characterisation and study of the properties of bioceramics, particularly bioactive sol-gel glasses to be included in drug release systems and biphasic materials. She passed away on June 1, 2002.

Antonio J. Salinas (left, bottom) was born in Madrid, Spain, in 1957. He studied Chemistry at the Universidad Complutense de Madrid (UCM) and received his PhD at the same University in 1992. He is associate professor at the Department of Inorganic Chemistry and Bioinorganic of the Faculty of Pharmacy (UCM). His current research field is the synthesis and characterisation of bioactive ceramics: gel glasses and glass ceramics, to be used in the osseous defects treatment.

MICROREVIEWS: This feature introduces the readers to the authors' research through a concise overview of the selected topic. Reference to important work from others in the field is included.

the case in silica glass. A common feature of both the crystalline − i.e., quartz − and the amorphous structures is that each oxygen ion links two tetrahedra, although forming a more open arrangement in the case of amorphous silica (Figure 1, b). Such a rather open structure facilitates the inclusion of cations referred to as network modifiers, and this feature allows a wide range of silica glasses to be obtained.

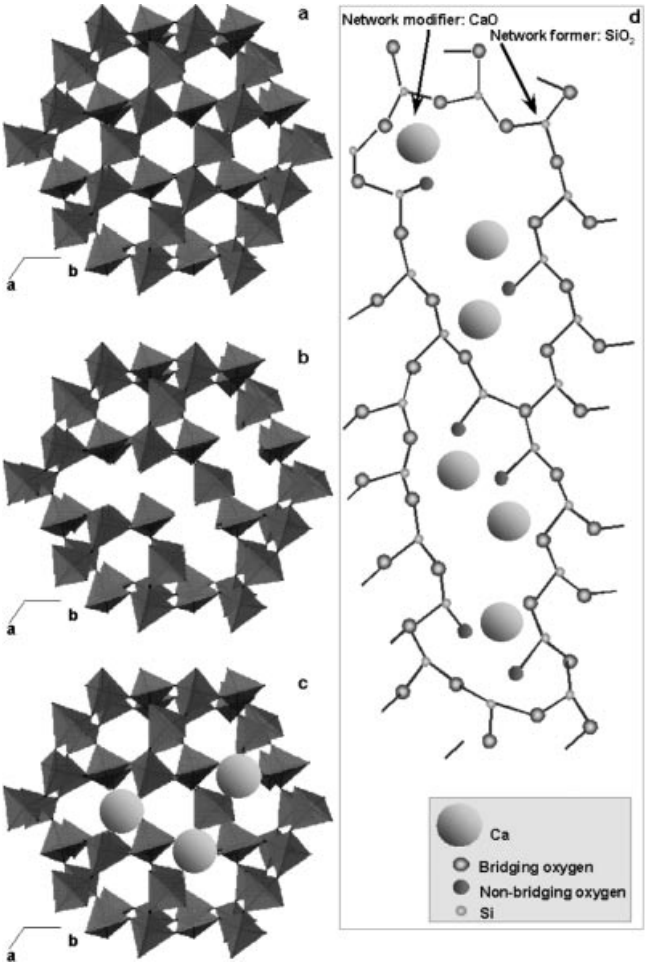

Figure 1. (a) Crystallised silica, (b) amorphous silica, (c) silica glass, (d) glassy network in two dimensions

The presence of cations such as Na^+, K^+ and Ca^{2+} (Figure 1, c) in the glass causes a discontinuity of the glassy network through the disruption of some Si−O−Si bonds. As a consequence, non-bridging oxygen is released. Figure 1, part d schematically depicts a glassy network in two dimensions. The network modifier in this case is an MO-type oxide, CaO, while the network former is SiO_2. Some Si atoms are bonded to other Si atoms through bridging oxygen, while others are coordinated through a non-bridging oxygen to the network of modifying ions. The purpose of the *network formers* is to build Si−O−Si bonds, while the *network modifiers* are there to break a proportion of those bonds, thus allowing the melt to solidify with a high degree of disorder. Its presence provides lower melting temperatures and viscosity values, reducing the economic costs of glass production, while ensuring a high degree of disorder.

This disordered structure, enhanced by the presence of network modifiers, gives rise to the high reactivity of these glasses in aqueous environments. This high reactivity is the main advantage of their application in periodontal repair and bone augmentation, as the reaction products obtained from these types of glasses and physiological fluids result in the crystallisation of the apatite-like phase, similar to the inorganic component of bones in vertebrate species.[3−9]

Bioactive glasses, from their beginnings in the 1970s, have reached a significant level of development, resulting since their discovery in the publication of several reviews on ceramics for medical applications, studying various aspects of their evolution.[11−18] This microreview reflects the more relevant results of our research in bioactive glasses.

2. Bioactive Glasses

Early bioactive glasses were prepared by the classic quenching of melts comprising SiO_2 and P_2O_5 as network formers and CaO and Na_2O as network modifiers.[1] This was the route followed for more than two decades in the synthesis of bioactive glasses.[3,19−24] In the early 1990s, sol-gel processing was introduced for the synthesis of bioactive glasses;[25] Figure 2 shows a scheme illustrating the main stages of the melting and sol-gel processes. The sol-gel route allows glasses of higher purity and homogeneity to be obtained, and the ranges of their compositions and textural properties to be expanded. In addition, all the steps in this route are carried out at temperatures notably lower than those required to obtain glasses by the melting method. It was therefore no longer necessary to include components intended to decrease the melting temperature (i.e., Na_2O), and the first bioactive gel glasses in the SiO_2·CaO·P_2O_5 system were obtained.

Our research group used the sol-gel route for preparation of bioactive glasses not only in the ternary SiO_2·CaO·P_2O_5 system,[26−43] but also in the quaternary SiO_2·CaO·P_2O_5·MgO[26,28,31,32,44] and the binary SiO_2·CaO[30,35,37,41−43,45−48] systems (see Table 1).

The addition of MgO to obtain quaternary gel glasses was performed in an attempt to improve the mechanical features of the glasses. The magnesium should be regarded as a network modifier, just as calcium, but it has different chemical behaviour and so substantial variations in the glass properties would be expected. Thus, Kokubo et al.[49] described the bioactive Apatite−Wollastonite glass-ceramic, based on an SiO_2·CaO·P_2O_5·MgO melt glass, with mechanical properties appreciably better than those of glasses.

The sol-gel method allows the ternary system to be simplified, P_2O_5 to be eliminated, and binary SiO_2·CaO bioglasses of a wide compositional range to be obtained. The objective of these studies was to determine the role of phosphorus in the gel glasses' bioactivity. This binary system can also help to understand the mechanism of bioactivity,

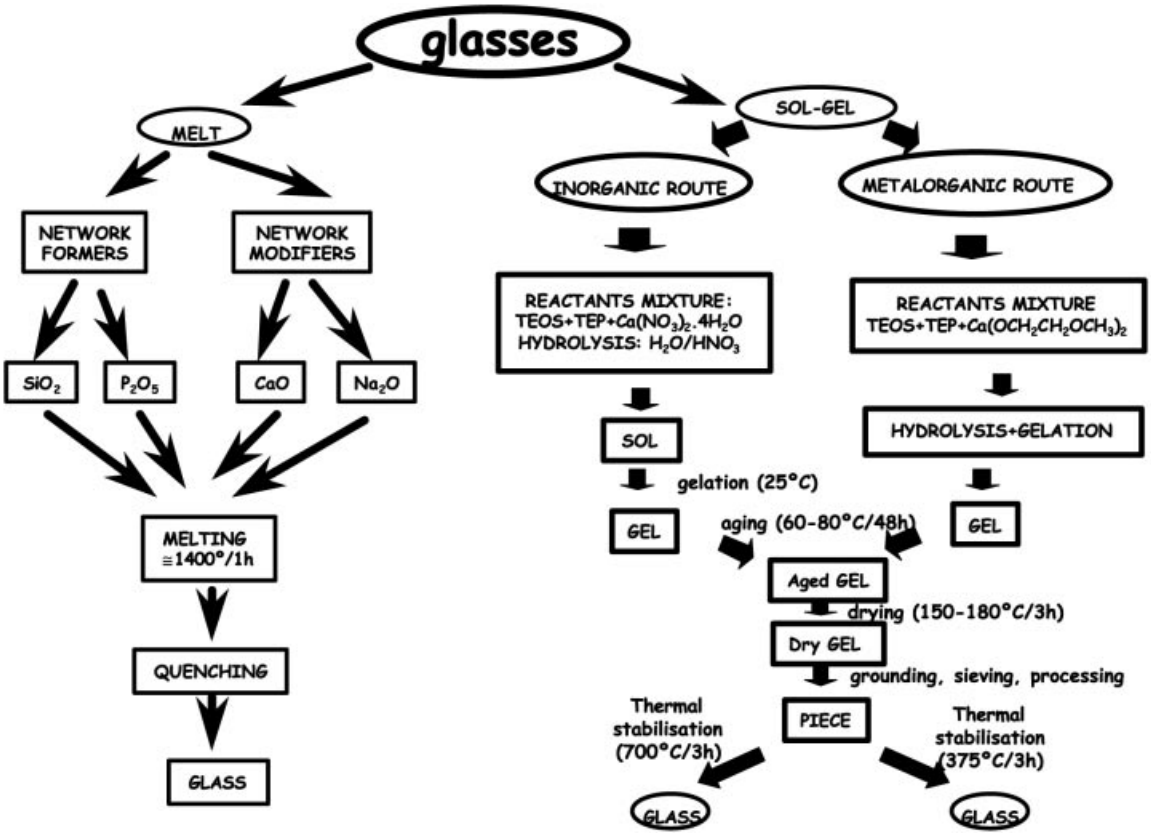

Figure 2. Diagram of the main stages in the melting and sol-gel processes (inorganic and metalorganic routes) to obtain bioactive glasses

since the phosphorus required for the apatite-like layer formation could now only originate from the assay solution.

In all cases, the syntheses of glasses were carried out by hydrolysis and polycondensation in the glass of stoichiometric amounts of the oxide precursors: tetraethyl orthosilicate (TEOS), triethyl phosphate (TEP), magnesium nitrate hexahydrate and calcium nitrate tetrahydrate (*inorganic route*) or calcium methoxyethoxide (*metalorganic route*),[39] by the scheme shown in Figure 2.

In the *inorganic route*, HNO_3 (2 N) was used to catalyse the TEOS and TEP hydrolyses, the (HNO_3 + H_2O/TEOS + TEP) molar ratio being constant and equal to 8. Reactants were added consecutively after 1-h intervals, with continuous stirring. The solution (*sol*) was poured into Teflon® containers, which were closed and kept at room temperature until gelation (*gel*) was reached (2−5 d depending on the *sol* composition). Ageing was achieved by a thermal treatment (70 °C/55 h) and the drying of the gel at 150 °C/72 h, after replacement of the container lid with another one with a small hole, allowing the gasses to leak. The dried gel was ground and sieved, and the 63−32 μm fractions were selected. Disks (13 mm diameter, 2 mm in height), were conformed by uniaxial (50 MPa) and isostatic (150 MPa) pressures on 0.5 g of dried gel powders. Nitrate elimination and material stabilisation was carried out at 700 °C/3 h, the temperature being determined by thermogravimetric analysis of the dried gels.

On the other hand, in view of the excellent bioactivity of the obtained gel glasses, we considered that their application field could be expanded through the preparation of new mixed materials, in which these glasses would be the bioactivity-inducing elements. We have thus obtained: (i) bioactive systems for controlled release of anti-inflammatory drugs and antibiotics, avoiding problems derived from implantation as bone substitutes, (ii) magnetic bioactive materials, for the treatment of osseous tumours by hyperthermia, and (iii) calcium phosphate based materials with improved kinetics for the formation of new apatite, thanks to the presence of the bioactive glass.

Finally, gel glasses have been used to prepare metallic substrate coatings (of Ti6Al4V) by dip-coating. These coatings allow the good mechanical properties of metals to be combined with the bioactivity of sol-gel glasses.

3. Ternary Compositions: SiO_2·CaO·P_2O_5 System

3.1 Characterisation of Glasses

Analyses of the compositions of gel glass by X-ray fluorescence (XRF) and energy dispersive X-ray spectroscopy (EDS) showed good agreement with the nominal compositions[26−43] (Table 1).

X-ray diffraction (XRD) characterisation confirmed the amorphous character of all the materials, but in some cases a diffuse maximum was observed at $2\theta \approx 32°$. This could

Table 1. Nominal compositions (mol %) of sol-gel glasses obtained by our research group

Glass	SiO_2	CaO	MgO	P_2O_5	Ref.
80S	80	16	–	4	[26,27,31,38]
80S17C	80	17	–	3	[30,35,37]
75S	75	21	–	4	[26,28,32,38]
76S	76	23	–	1	[39]
76SA	76	23	–	1	[39]
72.5S2.5P	72.5	25	–	2.5	[41,42]
70S	70	26	–	4	[29,26,40]
70S5P	70	25	–	5	[41,42]
77S	77	14	–	9	[43]
68S	68	23	–	9	[43]
65S	65	31	–	4	[26,28,32,38]
60S	60	36	–	4	[26,27,38,40]
58S	58	36	–	6	[34,38]
58S33	58	33	–	9	[43]
55S	55	41	–	4	[33,36]
80SM	80	12.8	3.2	4	[44]
80SM	80	13	3	4	[26,31]
80S7M	80	9	7	4	[31]
75SM	75	17	4	4	[26,28,32]
75SM	75	16.8	4.2	4	[44]
70SM	70	21	5	4	[26]
65SM	65	25	6	4	[26,28,32]
65SM	65	24.8	6.2	4	[44]
60SM	60	29	7	4	[26]
60SM	60	28.8	7.2	4	[44]
91S	91	–	–	9	[43]
90S10C	90	10	–	–	[48]
80S20C	80	20	–	–	[30,35,37,45–48]
75S25C	75	25	–	–	[41,42]
70S30C	70	30	–	–	[48]
60S40C	60	40	–	–	[48]
50S50C	50	50	–	–	[48]

be attributable to the more intense reflection of an apatite-like phase that could start to crystallise in the amorphous glass matrix.

The obtained Fourier-transform infrared (FTIR) spectra show bands attributable to the Si–O stretching vibrations (ν_a: ca. 1085 cm^{-1}; ν_s: ca. 802 cm^{-1}) and Si–O–Si bending vibrations (ca. 472 cm^{-1}). In addition, two low-intensity bands are registered at about 602 and 568 cm^{-1} and could be attributable to stretching vibrations of phosphate groups.

Characterisation by scanning electron microscopy (SEM) indicates that pieces of the glasses are made up of particle aggregates with a wide size distribution (ca. $1-25 \times 10^3$ nm) and with sharp edges, allowing numerous voids between them.

The textural properties (porosity and specific surface) were also determined,[32–34,38,42] by N_2 adsorption and intrusion mercury porosimetry. Figure 3 (see a) shows the nitrogen adsorption isotherms for the ternary, 60S, 65S, 75S and 80S gel glasses.[38] The inset shows the BET surface and mesoporous volume values obtained by this technique.

All the nitrogen adsorption isotherms can be identified as type IV isotherms with slight differences in the hysteresis loop.[50] Samples with SiO_2 contents under 70 mol % have an H1 type hysteresis loop in the mesoporous region (3–50 nm), characteristic of cylindrical pores with both sides open, with some narrow parts. In contrast, glasses with SiO_2 contents higher than 70 mol % present hysteresis loops of H2 type associated with inkbottle-like pores with variable size and narrow necks.

Figure 3, part b shows the pore volume as a function of the pore diameter in the macropore region (2×10^5 to 50 nm) obtained by mercury intrusion. The inset shows macropore diameter vs. SiO_2 content. As observed, the pore volume in this region increases when the SiO_2 content in the glasses decreases.

These results indicate that the textures of the sol-gel glasses in this system are determined by the relative amounts of the glass components. For the same contents in P_2O_5 (4 mol %), higher CaO percentages, and consequently lower SiO_2 contents, yield higher mesopore volumes. Simultaneously, pore diameter increases, whereas the surface area decreases. These results were explained by taking into account that increases in calcium content in the SiO_2 network increase the number of nonbonding oxygen atoms. A proportion of the micropores is therefore substituted by mesopores, producing a decrease in the specific surface.

It was observed that variations in the pore morphology parallel their modifications in volume and diameter. An increase in the pore size and volume joins the "inkbottle" pores together, producing cylindrical pores. A model presenting the transition in the pore morphology is depicted schematically in Figure 3, part c.

For constant CaO contents (25 mol %), however, the surface area increases and the pore diameter and volume decrease with increasing P_2O_5 content.[42] This was explained by considering that P_2O_5 bonds to calcium, decreasing the amount of this element that can interact with the silica network. An increase in the P_2O_5 content in the glass thus produces effects similar to those of a decrease in the CaO content (increasing the SiO_2 percentage).

Another point studied was the influence of the CaO precursor on the features of the sol-gel glasses obtained. With this as the objective, a glass composition was prepared from two different precursors (Figure 2): calcium nitrate tetrahydrate (*inorganic route*, 76S glass) and calcium methoxyethoxide (*metalorganic route*, 76SA glass).[39] 76SA has the following differences from 76S: it (i) was obtained in monolithic form, (ii) presented a lower pore volume (0.13 $cm^3 \times g^{-1}$ vs. 0.72 $cm^3 \times g^{-1}$ of 76S, obtained by Hg intrusion), and (iii) showed only one maximum (at 180 nm) in the pore size distribution, while 76S glass showed a bimodal distribution with maxima at 820 nm and 6 nm. Variations in texture can be explained by the porosity generated in the thermal treatment required for nitrate elimination in the synthesis of the 76S glass. This different textural properties give rise to different in vitro behaviour in the two glasses, as explained in the next section.

3.2 In Vitro Bioactivity Studies

There is a well-established relationship between the ability of a given material to form bonds with living tissues and its ability to grow an apatite-like layer when soaked in fluids mimicking human plasma, and so in vitro assays are pop-

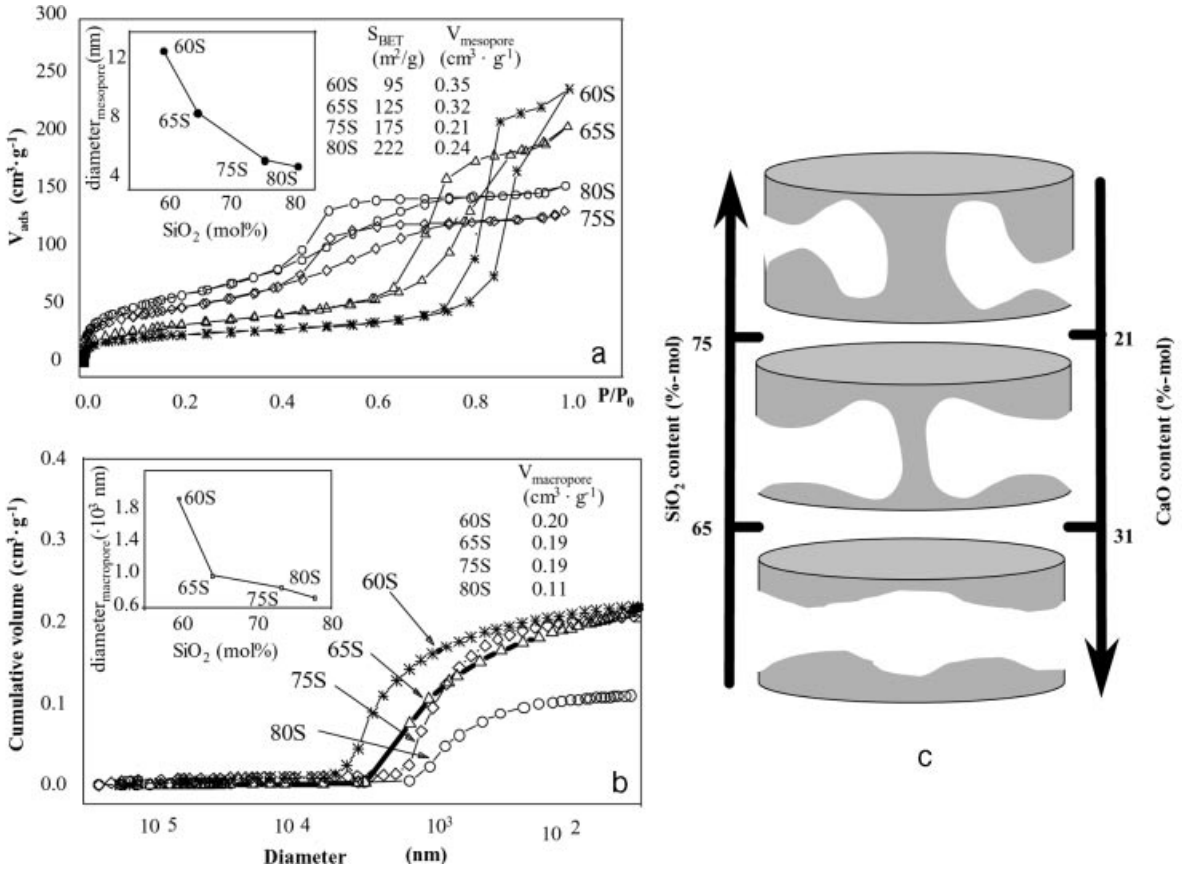

Figure 3. (a) N_2 adsorption isotherms of several $SiO_2 \cdot CaO \cdot P_2O_5$ sol-gel glasses; the inset shows the mesopore diameter versus SiO_2 content; BET surface and mesopore volume data are also included; (b) volume of intrusion Hg as a function of pore diameter; the inset shows the macropore diameter versus SiO_2 content; the macropore volume data are included; (c) model of the transition in the mesopore morphology as a function of the composition of the gel glasses

ular tools in the study of bioactivity of new candidate implant materials. In most of our research we have used the simulated body fluid (SBF) proposed by Kokubo et al.[7] SBF is an acellular, aqueous solution with an ionic composition that closely resembles that of human plasma, buffered to physiological pH (7.25−7.40) at 37 °C with a mixture of HCl/tris(hydroxymethyl)aminomethane. Figure 4 compares the ionic compositions of SBF and human blood plasma. Since this fluid contains Ca^{2+} and HPO_4^{2-} ions, it can be used to assess the in vitro bioactivity of a wide range of materials.

During the in vitro assays, the glass disks are soaked in SBF for time periods ranging from 1 h to 2 weeks. To homogenise our studies, to avoid effects due to volumetric differences, the relationship between the geometric areas of pieces and the volumes of solutions was 0.075 cm^{-1} in all cases. Disks are kept in a vertical position in a platinum scaffold (Figure 4). After the assays, pieces are washed with water and acetone and dried in air. Microorganism contamination of samples is avoided by performing all the manipulations inside a laminar flux cabinet and by filtering the SBF with a 0.22 μm Millipore® system.

In vitro bioactivity of glasses is evaluated by monitoring changes in pH and Ca^{II}, Si^{IV} and P^{V} concentrations in solution and by analysing the apatite layer formation on the surface of the pieces by XRD, FTIR, SEM-EDS, transmission electron microscopy (TEM) and electron diffraction (ED).

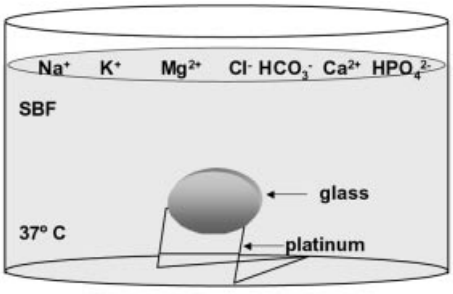

Ionic composition of SBF and Human Blood Plasma (mM)

	Na^+	K^+	Mg^{2+}	Ca^{2+}	Cl^-	HCO_3^-	HPO_4^{2-}	SO_4^{2-}
SBF	142.0	5.0	1.5	2.5	147.8	4.2	1.0	0.5
plasma	142.0	5.0	1.5	2.5	103.0	27.0	1.0	0.5

Figure 4. Schematic depiction of the in vitro bioactivity test; ion concentrations in SBF and in human blood plasma are also indicated

In general terms, as soaking time increases there is an increase in pH and in the Ca^{II} and Si^{IV} concentrations in SBF, whereas the P^{V} concentration in SBF decreases simultaneously. These effects are more pronounced in the first 12

h of assay and decrease after that. These variations agree with an exchange taking place between Ca^{2+} ions of the glass and H_3O^+ of the solution. This exchange favours the formation of Si−OH in the glass surface and increases the Ca^{2+} supersaturation in solution, inducing nucleation and crystallisation of apatite (Figure 5).

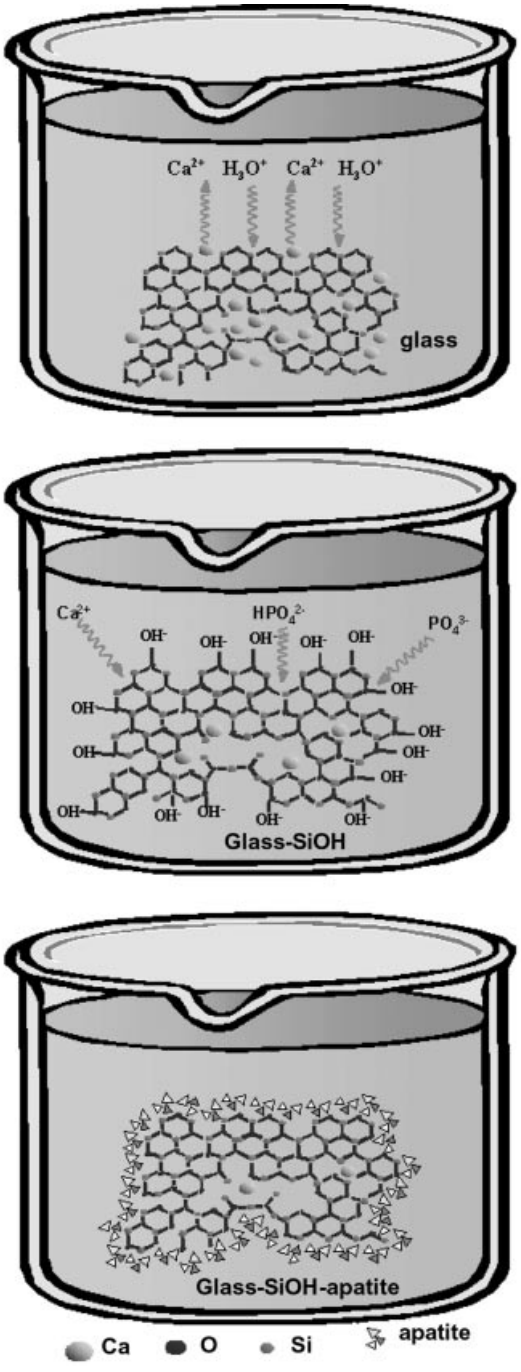

Figure 5. Depiction of the apatite formation mechanism as a function of the reactivity of bioactive glasses when in contact with physiological fluids, under in vitro conditions

Figure 6, part a shows the XRD diagrams of 60S glass before and after soaking for different periods in SBF. As the soaking time increases, diffraction maxima attributable to the more intense reflections of an apatite-like phase are registered. The intensities of these maxima increase with the immersion time as the apatite crystal size increases.

Figure 6, part b depicts FTIR spectra of 58S glass before and after soaking in SBF for different time periods. As the immersion time increases, the spectra develop bands attributable to the phosphate and carbonate groups, the intensities of these bands increasing with the soaking time. The presence of such bands shows that the material formed on the glass surface is hydroxycarbonate apatite (HCA), similar to biological apatites.[51,52]

SEM studies indicate that during the early soaking stages the glasses are totally coated by a layer of spheres of a diameter between 1 and 20×10^3 nm, identified by FTIR and EDS as amorphous calcium phosphate. For soaking times longer than 3−4 d, it was observed that the spheres were composed of numerous elongated particles (Figure 6, c). The times required for these processes varied with the gel glass composition but, in general, were lower for ternary gel glasses with high CaO contents.

The particles forming the spheres are made up of numerous crystalline aggregates, as confirmed by TEM (Figure 6, d). The correspondent ED diagram shows rings and diffraction maxima attributable to the more intense reflections of an apatite-like layer (Figure 6, e).[30] In addition, EDS analysis shows that the layer formed on 80S17C glass after 7 d in SBF is made up only of Ca, P and O (Figure 6, f).

The thickness of the newly formed layer can be studied by SEM, by cutting the pieces after the in vitro assays and applying the procedure shown in Figure 7. The EDS spectrum of the bulk glass (Figure 7, c) agrees with its nominal composition, whereas higher Ca and P concentrations and a lower Si content are detected in the layer, the thickness of which varies with glass composition and soaking time in SBF. For 55S glass, a thickness of 2×10^3 nm is measured after 15 h and increases up to a maximum value of 10×10^3 nm after 5 d of assay. In addition, the Ca/P molar ratio in the newly formed layer ranged between 1.4 and 1.7, within the common limit values for biological apatites.[53,54]

3.3 Texture − In Vitro Bioactivity Relationship in Sol-Gel Glasses

The formation of an Si-rich layer and a calcium phosphate layer on bioactive glasses is a well-established fact.[55−59] Figure 5 outlines the essential steps in the mechanism of formation of an apatite-like layer. The process takes place through the free surface of the glass, so those factors responsible for an increase in the specific surface of the initial glass also support an acceleration of the kinetics of this mechanism of chemical reactivity in bioactive glasses. This was in fact one of the main reasons to search for additional synthesis routes to these glasses, trying to enhance the specific surface and porosity of the final product.[60−64] The Si-rich layer is clearly seen on the bulk glass, and the calcium phosphate is seen as a light uppermost layer on the Si-rich gel.

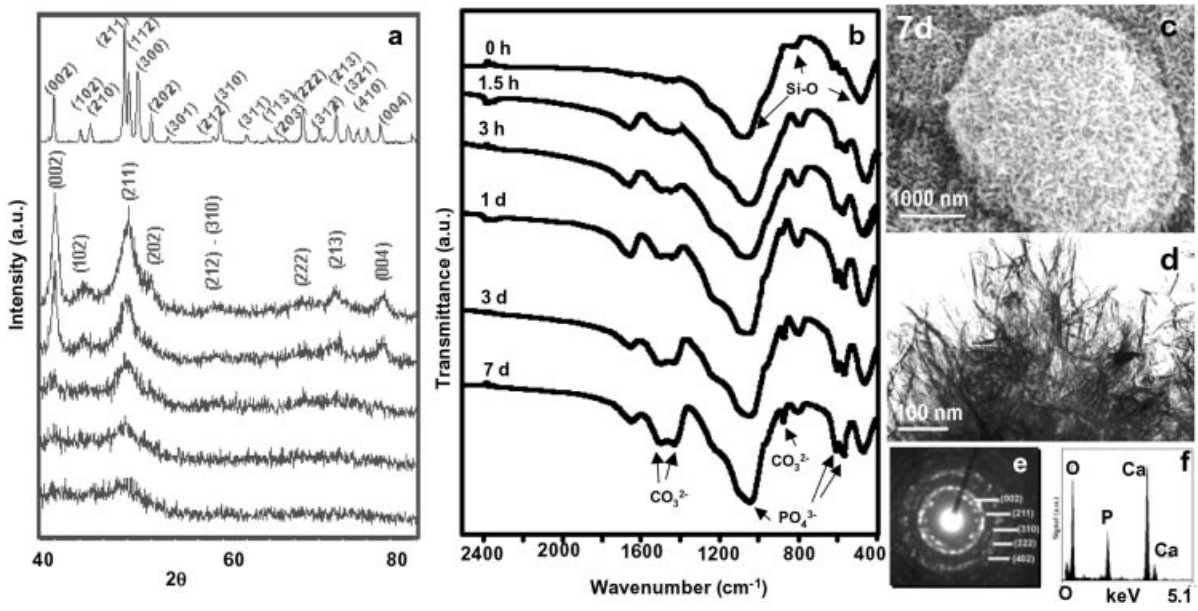

Figure 6. (a) XRD patterns of 70S before and after soaking different periods of time in SBF; an XRD pattern of hydroxyapatite is included as a reference; (b) FTIR spectra of 58S before and after soaking in SBF; (c) SEM micrographs; (d) TEM micrograph; (e) ED pattern, and (f) EDS spectra of 80S17C after a 7-d assay in SBF

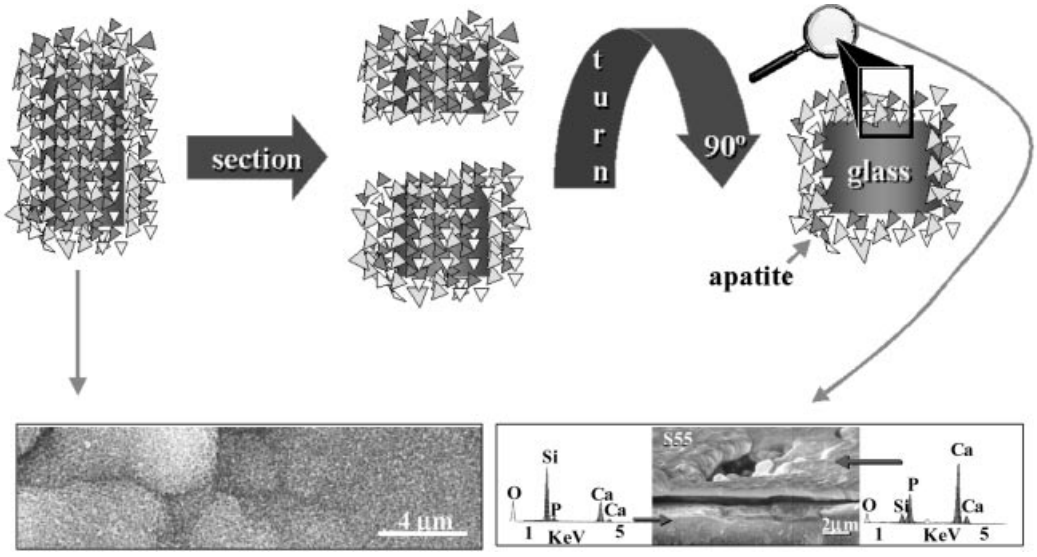

Figure 7. Schematic depiction of the sample treatment used to study the layer thickness by SEM-EDS; an SEM micrograph of 55S glass surface after 7 d soaking and SEM micrograph and EDS spectra of the inside of the glass and on the layer are also shown

High porosity in sol-gel glasses favours the formation of the apatite-like layer, since it facilitates rapid and massive release of Ca^{2+} ions from the glass into the solution. This release increases the Ca^{2+} saturation and pH in the medium, and induces silanol group (Si−OH) formation in the glass surface according to the following Equation:

$$2\ (Si{-}O)^{2-}\ Ca^{2+} + 2\ H_2O \rightarrow 2\ Si{-}OH + Ca^{2+} + 2\ OH^-$$

The formation of the silicon-rich layer is almost instantaneous, and it is covered within minutes by an amorphous phosphate layer, which in 2 or 3 d crystallises with an apatite structure. These processes also produce additional porosity, which facilitates the diffusion of more Ca^{2+} ions into the medium and the formation of new silanol groups. There are, however, other factors contributing to these reactions. CaO acts as network modifier, inducing instability in the system by provoking stress in the glassy network. Thus, generally speaking, a higher CaO content in the glass implies faster formation kinetics of the apatite phase.

The presence of CaO is also associated with a larger porosity of the glass, more so when introduced in the form of an inorganic salt such as $Ca(NO_3)_2$. In this context, a study on the differences between glasses in which CaO was included either as calcium alkoxide (76SA) or as calcium nitrate (76S) indicated that glasses obtained by the latter

method are more porous and less homogeneous.[39,65] In vitro studies of glasses indicate that both are bioactive. However, because of their better textural and structural properties, the layers formed on 76SA glass are thicker, more compact and more homogeneous.

3.4 Quantification of Bioactivity in SiO_2 Glasses

We have proposed a method to quantify and predict the bioactivity of silicate glasses;[40] it relates the SiO_2 network degradation with the factors that cause the formation of silanol groups on the glasses surface. As mentioned, these factors are mainly *composition* (amount of network modifiers: CaO, Na_2O, ...) and *textural* properties (surface area and porosity).

Preliminary studies show that the energy of activation (E_a) for the diffusion of $Si(OH)_4$, the soluble form of SiO_2, is closely related to the in vitro bioactivity of the studied glasses.[43] For melt and sol-gel silica glasses with in vitro bioactivity, it was observed that E_a for $Si(OH)_4$ diffusion after 6 h of assay is lower than 0.35 eV.

3.5 Sol-Gel Glasses Biocompatibility

The biocompatibility of these ternary sol-gel glasses was studied by means of osteoblast cell cultures.[41] It was observed that these materials allow and favour osseous cell growth.

In vivo studies involving the implantation of glass pieces in rabbit femur for time periods between 1 and 12 weeks were also performed;[66] the implants present excellent biocompatibility and osseous integration.

4. Quaternary Compositions: SiO_2·CaO·MgO·P_2O_5 System

As already indicated, the inclusion of certain quantities of MgO as a network modifier in the melt glass compositions can improve their mechanical properties. For that reason we performed the synthesis and an in vitro bioactivity study of sol-gel glasses of the SiO_2·MgO·P_2O_5 and SiO_2·CaO·MgO·P_2O_5 systems.

None of the compositions obtained in the SiO_2·MgO·P_2O_5 system show in vitro bioactivity. In the surface of SiO_2·CaO·MgO·P_2O_5 glasses, however, a phosphate-rich layer was formed after soaking in SBF at 37 °C.[26,28,31,32,44] In vitro studies show that the rate of formation of the new layer decreases with increasing magnesium content in glasses. Moreover, a whitlokite-like phase [β-$Ca_3(PO_4)_2$] was detected in the layer as well as the apatite, together with a noticeable increase in the layer thickness, reaching 20×10^3 nm for 80S7M glass.

In order to explain this decrease in the kinetics of layer formation in quaternary glasses, their textural properties were studied.[32,44] Increases in the MgO content were found to increase the surface area and pore volume, whereas the pore sizes remained almost constant. These differences are not sufficient to justify the strong inhibitory effect of MgO in the crystallisation and growth of apatite, since the opposite effect (that is, an increase in the apatite layer growth for larger surface areas) was observed in bioactive ternary SiO_2·CaO·P_2O_5 glasses.

Because of this, the surfaces of quaternary glasses were analysed by TEM-EDS. The study shows that the glasses are chemically heterogeneous at nanometric scales and that

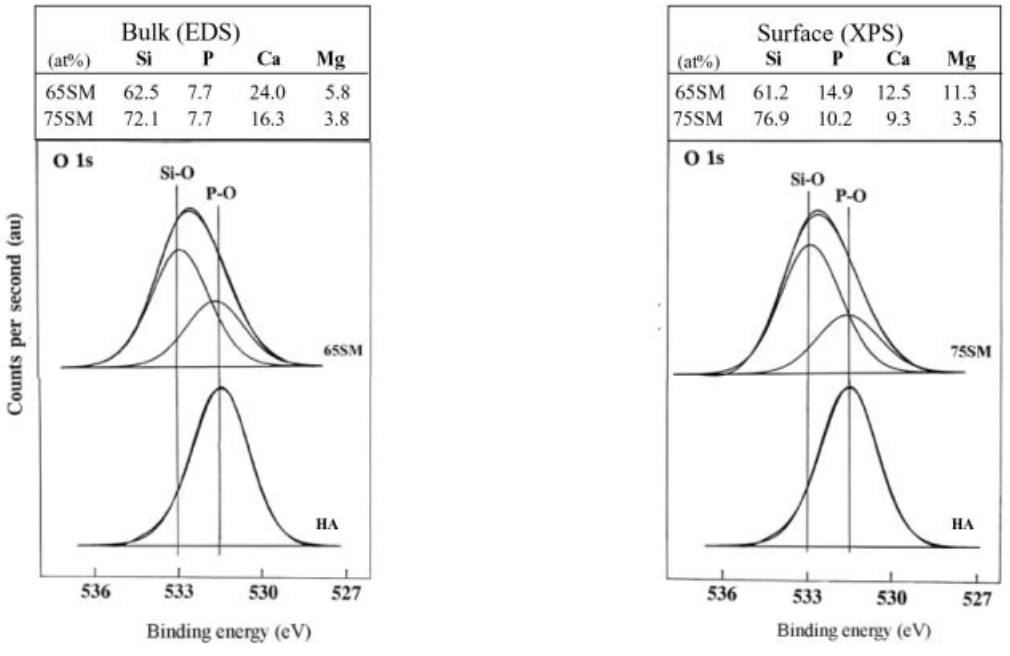

Figure 8. XPS spectra of oxygen 1s of the quaternary 65SM and 75SM glasses; hydroxyapatite spectra are included as reference; bulk (EDS) and surface (XPS) compositions of the glasses are also included

magnesium is always attached to Ca, P and Si, whereas pure calcium phosphate crystals were not detected. Therefore, Mg seems to inhibit the formation of calcium phosphate microdomains. These microdomains would eventually act as preferred centres for apatite crystallisation in Mg-free glasses, as they would offer a minimum interfacial energy for nucleation.[32]

To gain a deeper knowledge of the glass surface, a surface analysis technique, such as X-ray Photoelectron Spectroscopy (XPS), is needed. These studies show that the glasses' surfaces are richer in phosphorus and magnesium and poorer in calcium than the interiors (Figure 8).[32] Figure 8 shows the XPS spectra of O1s for 65SM and 75SM, together with that of hydroxyapatite (HA), included as a reference. The spectra of glasses can be deconvoluted into two components at 531.3 eV (P−O in HA) and 533.1 eV (Si−O).

Results from EDS-TEM and XPS studies suggest the existence of calcium-magnesium phosphate microdomains on the surface of quaternary glasses. Since the amount of calcium phosphate domains drastically decreased when MgO was included, this was regarded as the primary factor producing the bioactivity decrease in quaternary glasses containing magnesium.

5. Binary Compositions: SiO_2·CaO System

As already mentioned, addition of MgO to the SiO_2·CaO·P_2O_5 system modifies the textural properties and decreases the bioactivity of sol-gel glasses, while simultaneously increasing the complexity of the system. We therefore conjectured that the exclusion of a component of the ternary system, such as P_2O_5, might help understanding of the bioactivity mechanism in glasses, if the resultant glass was bioactive.

There are literature reports of bioactivity for SiO_2·CaO melt glasses with maximum SiO_2 contents of 65 mol %[67] (higher silica contents would produce phase separation by this synthesis method).

Our group has synthesised CaO·SiO_2 glasses with SiO_2 contents between 50 and 90 mol % by the sol-gel method.[42,45,48] In vitro bioactivity studies in all cases show the formation of an apatite-like layer. These results indicate that the presence of P_2O_5 in glasses of this system is not essential to ensure bioactivity, even at very high SiO_2 contents.

As with the ternary system, it was observed that the rate of formation of the new layer increases with the CaO content in the glasses.[30] In addition, in glasses with high CaO contents (40 and 50 mol %), calcite ($CaCO_3$) was also detected in the layer together with the apatite.

To understand the role of P_2O_5 in the glasses' bioactivity, the behaviour of an 80% SiO_2/20% CaO glass in SBF was compared with that of a ternary glass with identical silica content and 3% of P_2O_5.[30] Moreover, silicate glasses with identical CaO contents (25 mol %) and P_2O_5 contents of 0, 2.5 and 5 mol % were compared.[42]

The obtained results allow the conclusion that the presence of phosphorus retards the initial reactivity of glasses, defined as the time required for the initial formation of the amorphous calcium phosphate. Once some nuclei are formed, however, the growth of apatite crystals in the new layer is quicker and affords larger crystals when there is a small amount of P_2O_5 in the glass composition.

6. Procedures for the In Vitro Bioactivity Studies

During the in vitro studies described above, the assay solution was not renewed and so the ions released from the glass remain in the container. This method is termed *static* or *integral*. When materials with high reactivity in aqueous solutions are studied, however, ionic analysis of the solutions shows huge ionic concentration variations during the assay. As a result, some authors have proposed the so-called *differential* method,[5,6] in which the solution is renewed at predetermined intervals. For sol-gel glasses, our studies have shown that solution substitution should be at intervals so short that sample manipulations would affect the apatite formation process. For that reason, also to simulate the continuous flux of body fluids at the implant surface, we have proposed a new *dynamic* or *continuous* in vitro procedure, in which SBF is continuously renewed with the aid of a peristaltic pump. Figure 9 shows the scheme of the device used for *dynamic* in vitro assays.

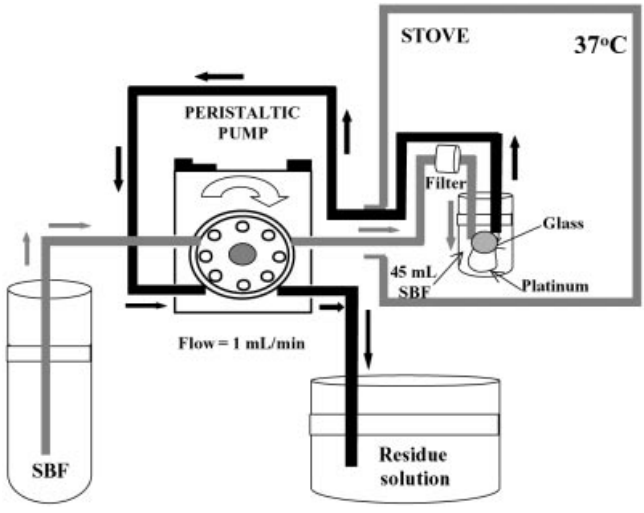

Figure 9. Representation of the dynamic procedure used for in vitro tests in SBF; a peristaltic pump continuously exchanges the assay solution to model the continuous flow of body fluids at the implant surface

This procedure was used for a bioactivity study of several glasses, results being compared with those obtained in *static* mode.[37,47] The use of a *dynamic* procedure allows complete bioactivity assays to be performed while keeping ionic concentration and pH almost equal to those of plasma. Fig-

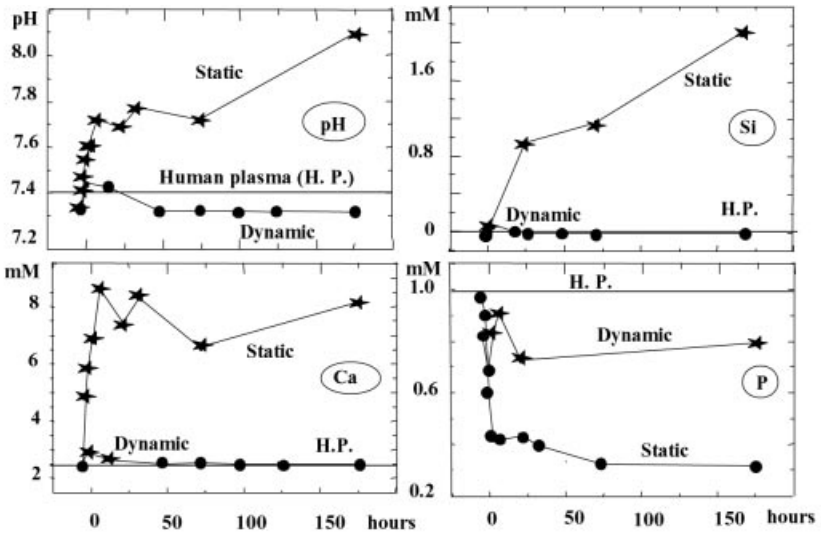

Figure 10. Variation of pH and Ca^{II}, P^{V} and Si^{IV} concentrations with soaking time in solution for 80S20C by use of static and dynamic in vitro procedures; the horizontal line in the figures indicates the values in human plasma

Table 2. Comparison between the two procedures used for in vitro studies of 80S20C and 80S17C sol-gel glasses

		Static	Dynamic
	SBF	Variations in solution after 7 d	
pH	7.30	8	7.30
Ca^{II} [mM]	2.5	8.5	2.5
P^{V} [mM]	1.0	0.3	0.8
Si^{IV} [mM]	0	2.1	0
		Variations in the layer	
Amorphous calcium phosphate		early formation	later formation
Apatite crystallisation		smaller crystals	bigger crystals
Layer composition		detected silicon	no silicon
Ca/P molar ratio		1.6	1.2

ure 10 shows variations with immersion time of Ca^{II}, P^{V}, Si^{IV} and pH in solution for 80S20C glass under *static* and *dynamic* conditions. Differences in solution composition, mainly pH, produced variations in the formation of calcium- and phosphorus-rich layers, shown schematically in Table 2. In *dynamic* mode, the amorphous phosphate layer was detected only after longer soaking times, but the size of the apatite crystals formed later is larger than in *static* mode. Regarding the layer composition, in contrast with static conditions, no traces of silicon were detected in *dynamic* mode and the Ca/P ratio was considerably lower (Figure 11, a). These differences were explained by the mechanism shown in Figure 11, b. The lower pH in *dynamic* mode (7.3) increases the HPO_4^{2-} ion concentration in solution compared with the static conditions under which the pH is close to 8. In this sense, use of the *dynamic* mode would favour the formation of calcium-deficient apatite, which might coexist with other calcium phosphates of lower Ca/P molar ratio.

7. Sol-Gel Glasses: Components of Mixed Materials

The excellent bioactivity of sol-gel glasses (SGGs) makes them potential candidates for osseous tissue regeneration. These glasses could be the optimal complement in systems for release of therapeutic action substances, such as antibiotics or anti-inflammatory agents, able to mitigate the problems originating from the material implantation.

The combination of these bioactive glasses with magnetic materials may also be an option for treatment of osseous tissues affected by tumours, since it should be possible to obtain bioactive and magnetic pieces capable of regenerating the bone, and to apply hyperthermia treatment. Moreover, the bioactive glass/hydroxyapatite (HA) combination can accelerate the bioactive response of HA. We have developed several SGG-polymer-drug, SGG-magnetic component and SGG-HA mixed materials, described below.

7.1 Sol-Gel Glass-Polymer-Drug

The study of systems for controlled release of drugs began with the synthesis of ceramic-polymer-drug materials including anti-inflammatory and antibiotic drugs.[68−73] In vitro studies showed that the release of the drug depends on its solubility and the piece matrix's porosity and capability to absorb liquid.

If a bioactive SSG is used as inorganic component in these systems,[74−77] a controlled release system, simultaneously bioactive, is produced. In this way, the osseous integration is improved and the drug release is favoured, due to the ionic interchange between the glass and medium.

On the other hand, the release of gentamicin from SSG implants was studied under in vivo conditions.[66] Gentamicin levels found in the organs analysed indicate that these

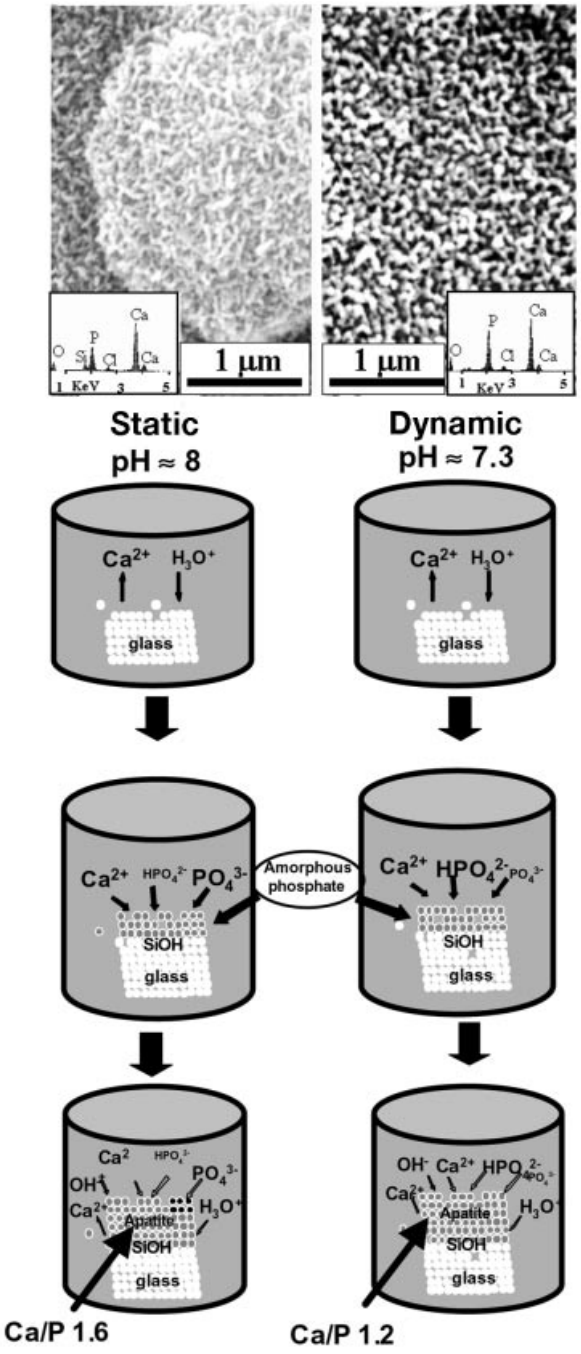

Figure 11. SEM micrographs and EDS patterns of 80S20C after 7 d soaking with use of static and dynamic in vitro bioactivity procedures and the proposed model to explain the different Ca/P molar ratio values obtained by EDS in the newly formed layer

implants are useful as drug release systems in bone during the 12 weeks of study.

7.2 Sol-Gel Glass-Magnetic Glass-Ceramic

The sensitivity of cancer cells to high temperatures was discovered 70 years ago, and the possibility of treating tumours by controlled heating has been studied since then. Nowadays, such therapy is termed *hyperthermia*. Among the techniques for application of this therapy, those of *interstitial hyperthermia* produce heat with the aid of devices directly implanted in the affected area. These devices can be magnetic materials, which will generate heat in an external alternating field, due to hysteresis losses or parasite currents. Heat is restricted to the desired volume without affecting the surrounding tissues.

Among those materials that have been proposed as *thermoseeds* in *interstitial hyperthermia*, magnetic glass-ceramics (MGCs) are interesting alternatives for the substitution and filling of osseous tissues exhibiting tumours.[78−82]

In our group we have studied the possibility of combining MGCs with bioactive glasses, synthesising biphasic materials presenting both properties. We have obtained several materials with varying proportions of the two components. Our studies showed that SGGs produce increases in the macro- and mesoporosity of the system, as well as higher reactivity in simulated body fluids, conferring high bioactivity on these biphasic materials.[83−84] However, the presence of SGGs seems partially to inhibit the incorporation of iron in the crystalline phases of the glass-ceramic, consequently decreasing the magnetic behaviour.[84]

7.3 Sol-Gel Glass-Hydroxyapatite

Hydroxyapatite (HA) is a highly suitable material for bone substitutions because it is not cytotoxic, presents excellent biocompatibility with living tissues, and is the material most similar to the mineral component of bone. However, the bioactivity of HA ceramics is lower than that of bioactive glasses.[85]

Our group has prepared and characterised SGG/HA biphasic materials offering more rapid kinetics of new apatite formation than pure HA.[86−88]

Figure 12 shows surface micrographs of 70S, HA and biphasic 70S/HA before and after soaking in SBF for different periods of time. As can be observed, the glass is coated by a layer of spheres after 7 d in SBF whereas the HA surface is not modified even after 45 d of immersion. Moreover, the biphasic 70S/HA is bioactive after only 12 h.

In addition, cross-sections of the biphasic materials before and after soaking for 3, 7 and 14 d in SBF were studied by SEM-EDS. The silicon content decreases from the inner part (ca. 30 μm) to the border, whereas Ca and P contents increase. The small amount of Si in the limit with the apatite-like layer obtained after 3 d of immersion is related to the lower thickness of this layer relative to those obtained after 7 or 14 d of treatment.

To visualise the newly formed layer better, Figure 13 shows the SEM micrographs, at different magnification, of the biphasic material surface after 7 d in SBF, as well as a cross section. The EDS spectrum of the new layer is also included. A layer thickness of approximately 3×10^3 nm and the absence of silicon in the new formed layer are observed.

8. Sol-Gel Glasses Coatings

Ceramic coatings of metallic pieces used as implants are of great interest because they combine the good mechanical

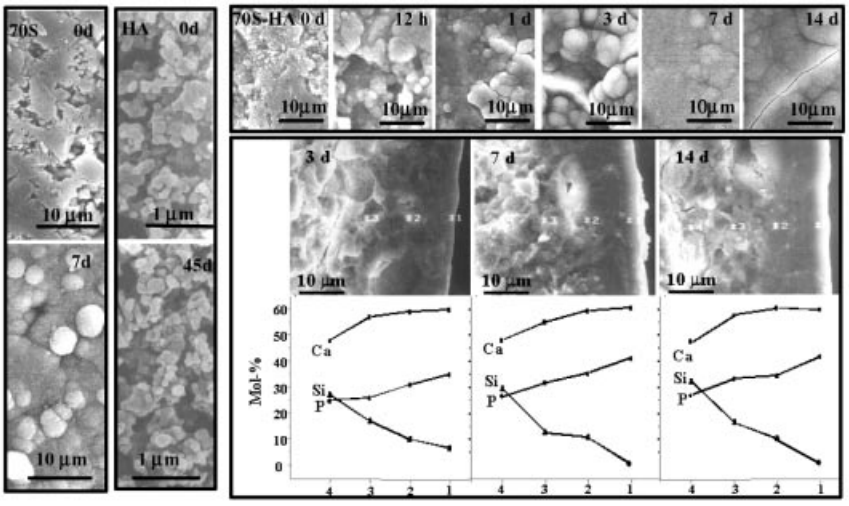

Figure 12. SEM micrographs of 70S glass, hydroxyapatite and 70S-HA biphasic material surfaces after SBF soaking several times; Ca, Si and P contents as a function of depth obtained by EDS in the transversal sections of biphasic material after SBF soaking for 3, 7 and 14 d are also included

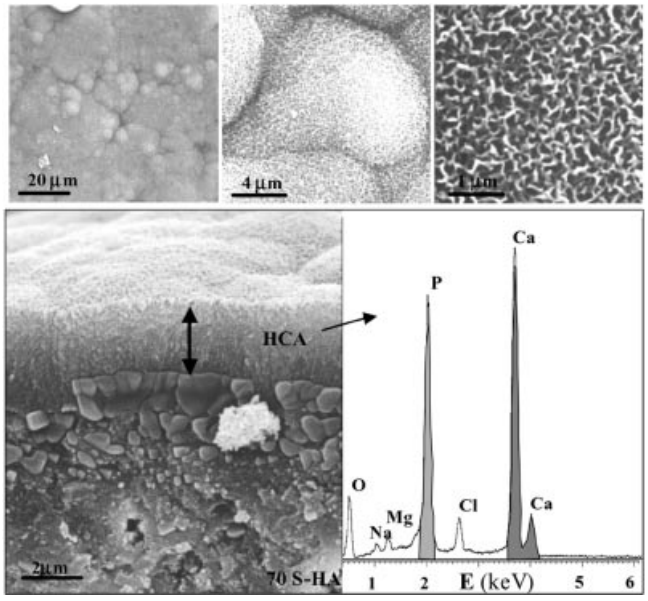

Figure 13. SEM micrographs of surface and a cross section of 70S-HA biphasic material after 7 d soaking; the EDS spectrum of the newly formed apatite layer is also included

properties of metals with the excellent biocompatibility and, in some cases, bioactivity of ceramics. At the same time, the metallic surface is protected from the biological medium, reducing corrosion and the release of ionic metals into the medium.

Sol-gel processing is ideal for the preparation of films by *dip-coating*. This method requires simple equipment and soft thermal treatments, and − its main advantage − allows a high degree of control over the microstructure and composition of the film, highly pure and homogeneous coatings being obtainable. *Dip-coating* technology is based on the capability of *sols* to form films on substrates introduced into them and extracted at a known rate. Many parameters affect the microstructure and thickness of the films, although the extraction velocity of substrate and the *sol* viscosity are strong limiting parameters. The extraction velocity must be lower than or equal to the gelling rate of the film in order to avoid flocculation processes and to maximise the adhesion to substrate.

Our group has prepared SiO_2·CaO system sol-gel coatings on metallic Ti6Al4V prostheses by *dip-coating*.[89] The characteristics of the method allow the porosity and thickness of coatings to be controlled by varying the properties of the starting solution. Figure 14 shows SEM and atomic force microscopy (AFM) micrographs of 80% SiO_2/20% CaO sol-gel coatings on a Ti6Al4V substrate.

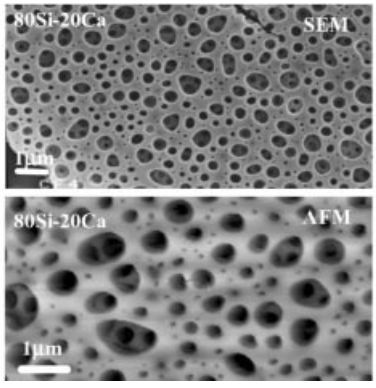

Figure 14. SEM and AFM micrographs of sol-gel glass coatings (80S20C glass) on metallic Ti6Al4V substrates

9. Future Expectations in Bioactive Glasses

From the advances in related medical technologies, bioactive materials appear to be entering a new stage of development in which they will have to be skilfully designed to exhibit a variety of new functions. These new functions include different mechanical properties, drug delivery capabil-

ity, the capability to activate proteins and/or cells for tissue regeneration and tissue engineering, biomimetics, nanotechnology, etc. Namely, there is significant increase in requirements for novel bioactive materials with different functions. To design a novel bioactive material successfully, the mechanism of bone-like apatite formation on the current bioactive materials should be specifically addressed and established.

Sol-gel glasses, as fibres or high-porosity monoliths, are good candidates with which to obtain biocompatible scaffolds for tissue engineering while maintaining mechanical properties during the resorption process. Growth factors (bone, platelet-derived, basic fibroblast) and polypeptides for their release can be included in the scaffolds.

On the other hand, the potential design of combinations of bioactive glasses and apatites could give very satisfactory results in terms of acceleration of the bioactivity of the apatites, which, due both to their composition and structure, are the ceramics most similar to the mineral component of the bone.

The new expectations on the field of hybrid organic/inorganic materials represent another route for future applications of bioactive glasses.

Acknowledgments

We would like to express our deepest gratitude to all our coworkers and friends who have contributed with their effort and thinking to these studies over the years. Financial support by the Spanish CICYT (MAT99-0466 and MAT01-1445-C02-01) is gratefully acknowledged.

[1] L. L. Hench, R. J. Splinter, W. C. Allen, T. K Greenlee, *J. Biomed. Mater. Res.* **1971**, *2*, 117−141.
[2] L. L. Hench, H. A. Paschall, *J. Biomed. Mater. Res.* **1973**, *7*, 25−42.
[3] L. L. Hench, *J. Am. Ceram. Soc.* **1991**, *74*, 1487−1510.
[4] C. G. Pantano, A. E. Clark, L. L. Hench, *J. Am. Ceram. Soc.* **1974**, *57*, 412−413.
[5] S. Radin, P. Ducheyne, B. Rothman, A. Conti, *J. Biomed. Mater. Res.* **1997**, *37*, 363−375.
[6] J. P. Zhong, D. C. Greenspan, in *Bioceramics 11* (Eds.: R. Z. LeGeros, J. P. LeGeros), World Scientific, Singapore, **1998**, p. 415−418.
[7] T. Kokubo, H. Kushitani, S. Sakka, T. Kitsugi, T. Yamamuro, *J. Biomed. Mater. Res.* **1990**, *24*, 721−734.
[8] P. Ducheyne, S. Brown, N. Blumenthal, L. L. Hench, A. Krajewski, G. Palavit, A. Ravaglioli, S. Steineman, S. Winderler, *Ann. N.Y. Acad. Sci.* **1988**, *523*, 257−263.
[9] T. Kokubo, H. Kushitani, C. Ohsuki, S. Sakka, T. Yamamura, *J. Mater. Sci.: Mater. Med.* **1992**, *3*, 79−83.
[10] K. Ohura, T. Nakamura, T. Yamamuro, T. Kokubo, Y. Ebisawa, Y. Kotoura, M. Oka, *J. Biomed. Mater. Res.* **1991**, *25*, 357−365.
[11] L. L. Hench, J. Wilson, *Science* **1984**, *226*, 630−636.
[12] G. Heimke, in *Handbook of Biomaterials Evaluation* (Ed.: A. F. Von Recum), Macmillan Publishing Company, New York, **1986**, p. 38−54.
[13] T. Kokubo, *J. Ceram. Soc. Jpn.* **1991**, *99*, 965−973.
[14] P. Ducheyne, *MRS Bulletin* **1998**, November 23, p. 43−49.
[15] L. L. Hench, T. Kokubo, in *Handbook of Biomaterials Properties* (Eds.: J. Black, G. Hastings), Chapman and Hall, London, **1998**, p. 355−363.
[16] M. Vallet-Regí, *J. Chem. Soc., Dalton Trans.* **2001**, 97−108.
[17] H. M. Kim, *J. Ceram. Soc. Jpn.* **2001**, *109*, S49−S57.
[18] L. L. Hench, J. M. Pollack, *Science* **2002**, *295*, 1014−1017.
[19] L. L. Hench, E. C. Ethridge, in *Biomaterials, An Interfacial Approach*, Academic Press, New York, **1982**, p. 139−148.
[20] Ö. H. Andersson, K. H. Karlsson, K. Kangasniemi, A. Yli-Urpo, *Glastech. Ber.* **1988**, *61*, 300−305.
[21] B. A. Blencke, H. Brömer, K. Deutcher, *J. Biomed. Mater. Res.* **1978**, *12*, 307−316.
[22] T. Kokubo, M. Shigematsu, Y. Nagashima, M. Tashiro, T. Nakamura, T. Yamamuro, S. Higashi, *Bull. Inst. Chem. Res. Kyoto Univ.* **1982**, *60*, 260−268.
[23] W. Vogel, W. Holland, *Angew. Chem. Int. Ed. Engl.* **1987**, *26*, 527−544.
[24] R. D. Rawlings, *J. Mater. Sci. Lett.* **1992**, *11*, 1340−1347.
[25] R. Li, A. E. Clark, L. L. Hench, *J. Appl. Biomat.* **1991**, *2*, 231−239.
[26] M. Vallet-Regí, F. Balas, M. Gil, E. Nogueroles, A. Romero, J. Román, A. J. Salinas, C. V. Ragel, in *Non-crystalline & nanoscale Materials* (Eds.: J. Rivas, M. A. Lopez Quintela), World Scientific, Singapore, **1998**, p. 55−60.
[27] A. J. Salinas, J. Román, M. Vallet-Regí, P. Fernández, J. Piqueras, in *Bioceramics* 11 (Eds.: R. Z. LeGeros, J. P. LeGeros), World Scientific, Singapore, **1998**, p. 707−710.
[28] F. Balas, J. Pérez-Pariente, M. Vallet-Regí, in *Bioceramics* 11 (Eds.: R. Z. LeGeros, J. P. LeGeros), World Scientific, Singapore, **1998**, p. 125−128.
[29] M. Vallet-Regí, A. M. Romero, C. V. Ragel, R. Z. LeGeros, *J. Biomed. Mater. Res.* **1999**, *44*, 416−421.
[30] M. Vallet-Regí, I. Izquierdo-Barba, A. J. Salinas, *J. Biomed. Mater. Res.* **1999**, *46*, 560−565.
[31] M. Vallet-Regí, A. J. Salinas, J. Román, M. Gil, *J. Mater. Chem.* **1999**, *9*, 515−518.
[32] J. Pérez-Pariente, F. Balas, M. Vallet-Regí, *Chem. Mater.* **2000**, *12*, 750−755.
[33] M. Vallet-Regí, A. Rámila, *Chem. Mater.* **2000**, *12*, 961−965.
[34] M. Vallet-Regí, D. Arcos, J. Pérez-Pariente, *J. Biomed. Mater. Res.* **2000**, *51*, 23−28.
[35] M. Vallet-Regí, J. Pérez-Pariente, I. Izquierdo-Barba, A. J. Salinas, *Chem. Mater.* **2000**, *12*, 3770−3775.
[36] A. Rámila, M. Vallet-Regí, *Biomaterials* **2001**, *22*, 2301−2306.
[37] A. J. Salinas, M. Vallet-Regí, I. Izquierdo-Barba, *J. Sol-Gel. Sci. Tech.* **2001**, *21*, 13−25.
[38] F. Balas, D. Arcos, J. Pérez-Pariente, M. Vallet-Regí, *J. Mater. Res.* **2001**, *16*, 1345−1348.
[39] A. Rámila, F. Balas, M. Vallet-Regí, *Chem. Mater.* **2002**, *14*, 542−548.
[40] D. Arcos, D. Greenspan, M. Vallet-Regí, *Chem. Mater.* **2002**, *14*, 1515−1522.
[41] M. Vallet-Regí, A. I. Martin, A. J. Salinas, N. Olmo, J. Turnay, M. A. Lizarbe, *Biol. Cell*, **2001**, *93*, 328−329.
[42] A. J. Salinas, A. I. Martín, M. Vallet-Regí, *J. Biomed. Mater. Res.* **2002**, *61*, 524−532.
[43] D. Arcos, D. Greenspan, M. Vallet-Regí, *J. Biomed. Mater. Res.*, in press.
[44] J. Pérez-Pariente, F. Balas, J. Román, A. J. Salinas, M. Vallet-Regí, *J. Biomed. Mater. Res.* **1999**, *47*, 170−175.
[45] I. Izquierdo-Barba, A. J. Salinas, M. Vallet-Regí, *J. Biomed. Mater. Res.* **1999**, *47*, 243−250.
[46] J. Pérez-Pariente, I. Izquierdo-Barba, J. L. García-Fierro, A. J. Salinas, M. Vallet-Regí, in *Bioceramics 12* (Eds.: H. Ohgushi, G. W. Hastings, T. Yoshikawa), World Scientific, Singapore, **1999**, p. 173−176.
[47] I. Izquierdo-Barba, A. J. Salinas, M. Vallet-Regí, *J. Biomed. Mater. Res.* **2000**, *51*, 191−199.
[48] A. Martínez, I. Izquierdo-Barba, M. Vallet-Regí, *Chem. Mater.* **2000**, *12*, 3080−3088.
[49] T. Kokubo, M. Shigematsu, Y. Nagashisma, M. Tashiro, T. Nakamura, T. Yamamuro, S. Higashi, *Bull. Inst. Chem. Res., Kyoto Univ.* **1982**, *60*, 260−268.
[50] S. J. Gregg, K. S. W. Sing, in *Adsorption, surface area and porosity*, Academic Press, New York, **1982**.

[51] R. Z. LeGeros, *Prog. Crystal Growth Charact.* **1981**, *4*, 1−45.
[52] R. Z. LeGeros, J. P. LeGeros, O. R. Trautz, E. Klein, *Dev. Appl. Spectrosc.* **1970**, *7B*, 13−22.
[53] A. Ravaglioli, A. Krajewski, G. C. Celoti, A. Piancastelli, B. Bacchini, L. Montanari, G. Zama, L. Piombi, *Biomaterials* **1996**, *17*, 617−622.
[54] C. Rey, A. Hina, A. Tofighi, M. J. Glimcher, *Cells Mater.* **1995**, *5*, 345−356.
[55] L. L. Hench, C. G. Pantano, P. J. Buscemi, D. C. Greenspan, *J. Biomed. Mater. Res.* **1977**, *11*, 267−281.
[56] Ö. H. Andersson, K. H. Karlsson, I. Kangasniemi, *J. Non-Cryst. Solids* **1990**, *119*, 290−296.
[57] E. Schepers, P. Ducheyne, De Clercq, *J. Biomed. Mater. Res.* **1989**, *23*, 735−742.
[58] Ö. H. Anderson, I. Kangasniemi, *J. Biomed. Mater. Res.* **1991**, *25*, 1019−1030.
[59] K. Ohura, T. Nakamura, T. Yamamuro, Y. Ebisawa, T. Kokubo, Y. Kotoura, M. Oka, *J. Mater. Sci. Mater. Med.* **1992**, *3*, 95−100.
[60] R. Li, A. E. Clark, L. L. Hench, in *Chemical Processing of Advanced Materials* (Eds.: L. L. Hench, J. K. West), John Wiley & Sons, Inc., New York, **1992**, p. 627−633.
[61] P. Li, K. Nakanish, T. Kokubo, K. De Groot, *Biomaterials* **1993**, *14*, 963−968.
[62] M. M. Pereira, A. E. Clark, L. L. Hench, *J. Am. Ceram. Soc.* **1995**, *78*, 2463−2468.
[63] M. M. Pereira, L. L. Hench, *J. Sol-Gel Sci. Tech.* **1996**, *7*, 59−68.
[64] M. M. Pereira, A. E. Clark, L. L. Hench, *J. Biomed. Mater. Res.* **1994**, *28*, 693−698.
[65] T. Peltola, M. Jokinen, H. Rahiala, E. Levänen, J. B. Rosenhold, I. Kangasniemi, A. Yli-Urpo, *J. Biomed. Mater. Res.* **1999**, *44*, 12−21.
[66] L. Meseguer-Olmo, M. J. Ros-Nicolas, M. Clavel-Sainz, V. Vicente-Ortega, M. Alcaraz-Baños, A. Lax-Pérez, D. Arcos, C. V. Ragel, M. Vallet-Regí, *J. Biomed. Mater. Res.* **2002**, *61*, 458−465.
[67] Y. Ebisawa, T. Kokubo, K. Ohura, T. Yamamuro, *J. Mater. Sci. Mater. Med.* **1990**, *1*, 239−244.
[68] D. Arcos, M. V. Cabañas, C. V. Ragel, M. Vallet-Regí, J. San Román, *Biomaterials* **1997**, *18*, 1235−1242.
[69] S. Granado, C. V. Ragel, V. Cabañas, J. San Román, M. Vallet-Regí, *J. Mater. Chem.* **1997**, *7*, 1581−1585.
[70] M. Vallet-Regí, S. Granado, D. Arcos, M. Gordo, M. V. Cabañas, C. V. Ragel, A. J. Salinas, A. L. Doadrio, J. San Román, *J. Biomed. Mat. Res.* **1998**, *39*, 423−428.
[71] M. Vallet-Regí, M. Gordo, C. V. Ragel, M. V. Cabañas, J. San Román, *Solid State Ionics* **1997**, *101−103*, 887−892.
[72] R. P. del Real, S. Padilla, M. Vallet-Regí, *J. Biomed. Mater. Res.* **2000**, *52*, 1−7.
[73] S. Padilla, R. P. del Real, M. Vallet-Regí, *J. Control Release* **2002**, *83*, 343−352.
[74] C. V. Ragel, M. Vallet-Regí, *J. Biomed. Mater. Res.* **2000**, *51*, 424−429.
[75] D. Arcos, C. V. Ragel, M. Vallet-Regi, *Biomaterials* **2001**, *22*, 701−708.
[76] S. Ladrón de Guevara, C. V. Ragel, M. Vallet-Regí, *Biomaterials*, submitted.
[77] A. Rámila, R. P. del Real, R. Marcos, P. Horcajada, M. Vallet-Regí, *J. Sol-Gel Sci. Tech.*, **2003**, *26*, 1195−1198.
[78] K. Ohura, M. Ikenaga, T. Nakamura, T. Yamamuro, Y. Ebisawa, T. Kokubo, Y. Kotoura, M. Oka, *J. Appl. Biomater.* **1991**, *2*, 153−159.
[79] Y. Ebisawa, Y. Sugimoto, T. Hayashi, T. Kokubo, K. Ohura, T. Yamamuro, *J. Ceram. Soc. Jpn.* **1991**, *99*, 7−13.
[80] M. Ikenaga, K. Ohura, T. Yamamuro, Y. Kotoura, M. Oka, T. Kokubo, *J. Orthop. Res.* **1993**, *11*, 849−855.
[81] Y. Ebisawa, F. Miyaji, T. Kokubo, K. Ohura, T. Nakamura, *J. Ceram. Soc. Jpn.* **1997**, *105*, 947−951.
[82] Y. Ebisawa, F. Miyaji, T. Kokubo, K. Ohura, T. Nakamura, *Biomaterials* **1997**, *18*, 1277−1284.
[83] D. Arcos, R. P. del Real, M. Vallet-Regí, *Biomaterials* **2002**, *23*, 2151−2158.
[84] D. Arcos, R. P. del Real, M. Vallet-Regí. *J. Biomed. Mater. Res.*, in press.
[85] H. Oonishi, L. L. Hench, J. Wilson, F. Sugihara, E. Tsuji, M. Matsuura, S. Kin, T. Yamamoto, S. Mizokawa, *J. Biomed. Mater. Res.* **2000**, *51*, 233−237.
[86] C. V. Ragel, M. Vallet-Regí, L. Rodríguez-Lorenzo, *Biomaterials* **2002**, *23*, 1865−1872.
[87] A. Ramila, S. Padilla, B. Muñoz, M. Vallet-Regí, *Chem. Mater.* **2002**, *14*, 24−39.
[88] M. Vallet-Regí, A. Ramila, S. Padilla, B. Muñoz. *J. Biomed. Mater. Res.*, in press
[89] I. Izquierdo-Barba, M. Vallet-Regí, J. M. Rojo, E. Blanco, L. Esquivias, *J. Sol-Gel Sci. Tech.*, **2003**, *26*, 1179−1182.

Received June 17, 2002
[I02312]